2017

Monitoring Early-Stage Protein Aggregation by an Aggregation-Induced Emission Fluorogen

Manjeet Kumar
Australian National University

Yuning Hong
University of Melbourne, La Trobe University

David C. Thorn
Australian National University

Heath Ecroyd
University of Wollongong, heathe@uow.edu.au

John A. Carver
Australian National University, john.carver@anu.edu.au

Publication Details

Kumar, M., Hong, Y., Thorn, D. C., Ecroyd, H. & Carver, J. A. (2017). Monitoring Early-Stage Protein Aggregation by an Aggregation-Induced Emission Fluorogen. Analytical Chemistry, 89 (17), 9322-9329.

Monitoring Early-Stage Protein Aggregation by an Aggregation-Induced Emission Fluorogen

Abstract

Highly ordered protein aggregates, termed amyloid fibrils, are associated with a broad range of diseases, many of which are neurodegenerative, for example, Alzheimer's and Parkinson's. The transition from soluble, functional protein into insoluble amyloid fibril occurs via a complex process involving the initial generation of highly dynamic early stage aggregates or prefibrillar species. Amyloid probes, for example, thioflavin T and Congo red, have been used for decades as the gold standard for detecting amyloid fibrils in solution and tissue sections. However, these well-established dyes do not detect the presence of prefibrillar species formed during the early stages of protein aggregation. Prefibillar species have been proposed to play a key role in the cytotoxicity of amyloid fibrils and the pathogenesis of neurodegenerative diseases. Herein, we report a novel fluorescent dye (bis(triphenylphosphonium) tetraphenylethene (TPE-TPP)) with aggregation-induced emission characteristics for monitoring the aggregation process of amyloid fibrils. An increase in TPE-TPP fluorescence intensity is observed only with ordered protein aggregation, such as amyloid fibril formation, and not with stable molten globules states or amorphously aggregating species. Importantly, TPE-TPP can detect the presence of prefibrillar species formed early during fibril formation. TPE-TPP exhibits a distinctive spectral shift in the presence of prefibrillar species, indicating a unique structural feature of these intermediates. Using fluorescence polarization, which reflects the mobility of the emitting entity, the specific oligomeric pathways undertaken by various proteins during fibrillation could be discerned. Furthermore, we demonstrate the broad applicability of TPE-TPP to monitor amyloid fibril aggregation, including under diverse conditions such as at acidic pH and elevated temperature, or in the presence of amyloid inhibitors.

Disciplines

Medicine and Health Sciences

Publication Details

Kumar, M., Hong, Y., Thorn, D. C., Ecroyd, H. & Carver, J. A. (2017). Monitoring Early-Stage Protein Aggregation by an Aggregation-Induced Emission Fluorogen. Analytical Chemistry, 89 (17), 9322-9329.

Monitoring Early-stage Protein Aggregation by an Aggregation-Induced Emission Fluorogen

Manjeet Kumar,[†] Yuning Hong,[‡,#,*] David C. Thorn,[†] Heath Ecroyd[§] and John A. Carver[†,*]

[†]Research School of Chemistry, The Australian National University, Acton, ACT 2601 Australia

[‡]Department of Chemistry and Physics, La Trobe Institute for Molecular Science, La Trobe University, Melbourne, VIC 3086 Australia

[#]School of Chemistry, The University of Melbourne, Parkville, VIC 3010 Australia

[§]School of Biological Sciences and the Illawarra Health and Medical Research Institute, University of Wollongong, NSW 2522 Australia

*Email: Y.Hong@latrobe.edu.au (Y.H.) or john.carver@anu.edu.au (J.C.)

ABSTRACT: Highly ordered protein aggregates, termed amyloid fibrils, are associated with a broad range of diseases, many of which are neurodegenerative, for example Alzheimer's and Parkinson's. The transition from soluble, functional protein into insoluble amyloid fibril occurs via a complex process involving the initial generation of highly dynamic early-stage aggregates or prefibrillar species. Amyloid probes, for example thioflavin T and Congo red, have been used for decades as the gold standard for detecting amyloid fibrils in solution and tissue sections. However, these well-established dyes do not detect the presence of prefibrillar species formed during the early stages of protein aggregation. Prefibillar species have been proposed to play a key role in the cytotoxicity of amyloid fibrils and the pathogenesis of neurodegenerative diseases. Herein, we report a novel fluorescent dye (TPE-TPP) with aggregation-induced emission characteristics for monitoring the aggregation process of amyloid fibrils. An increase in TPE-TPP fluorescence intensity is observed only with ordered protein aggregation, such as amyloid fibril formation, and not with stable molten globules states or amorphously aggregating species. Importantly, TPE-TPP can detect the presence of prefibrillar species formed early during fibril formation. TPE-TPP exhibits a distinctive spectral shift in the presence of prefibrillar species, indicating a unique structural feature of these intermediates. Using fluorescence polarization, which reflects the mobility of the emitting entity, the specific oligomeric pathways undertaken by various proteins during fibrillation could be discerned. Furthermore, we demonstrate the broad applicability of TPE-TPP to monitor amyloid fibril aggregation, including under diverse conditions such as at acidic pH and elevated temperature, or in the presence of amyloid inhibitors.

INTRODUCTION

Fluorescence-based techniques have been widely used to study protein structure due to their ease of application, flexibility and non-invasive nature [1]. In particular, dye-based assays have significantly enhanced our understanding of the complex conformational transition of soluble ordered/disordered proteins and peptides into insoluble β-sheet rich species, commonly known as amyloid fibrils. The aggregation of proteins or peptides into amyloid fibrils is a pathological hallmark of more than 50 human disorders, including Alzheimer's, Parkinson's and dialysis-related amyloidosis [2,3]. In contrast, amyloid fibrils with essential biological activities, often termed functional amyloid, have been reported [4]. In general, protein and peptide aggregation is not the direct conversion of soluble monomers to insoluble fibrils. Instead, multiple processes may be involved including the generation of transient, intermediately folded or unfolded states and oligomers (commonly known as prefibrillar species) that act as primary nuclei for further fibril growth [5]. These small oligomeric species are considered to be the dominant cytotoxic forms of misfolded proteins [6,7]. However, *in situ* and *ex situ* identification and characterisation of early-stage aggregates are difficult because they are generally heterogeneous, are present in minute quantities for a limited time, and are highly dynamic in nature [8]. Congo red and thioflavin T (ThT) are the most commonly used dyes in the study of protein aggregation associated with diseases. The green birefringence from Congo red under polarized light and the enhanced fluorescence of ThT are indicative of the presence of amyloid fibrils. Assays based on Congo red and ThT, however, are not able to detect the presence of early-stage aggregates [9-13]. More recently, penta-formylthiophene acetic acid, 9-(dicyanovinyl)-julolidine, Nile red, BODIPY-oligomer, *N*-aryl amino naphthalene sulfonate and its analogue, and tryptophanol have been used for the identification of prefibrillar species of various fibril-forming peptides and proteins [14-19], but most of these are specific to particular amyloid proteins. Therefore, novel probes that have broad applicability to report on the presence of prefibrillar species are desirable.

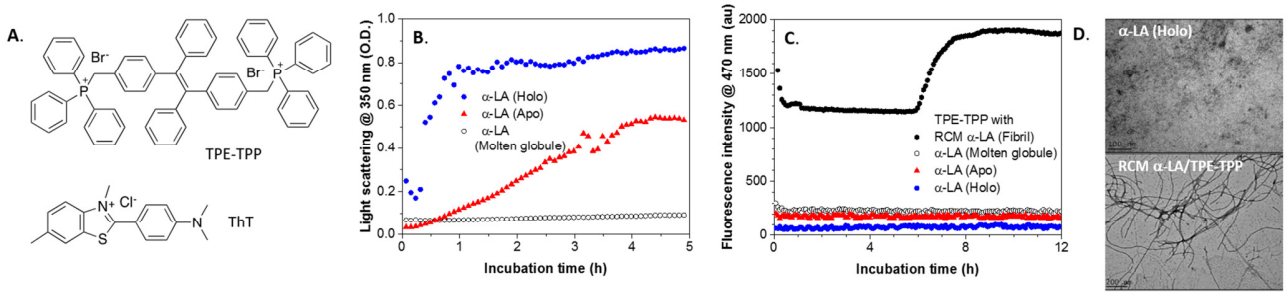

Figure 1. Fluorescence response of TPE-TPP to different forms of α-LA. (A) Structure of TPE-TPP (top panel) and ThT (bottom panel). (B) Time-course turbidity at 350 nm of molten globule (black open circle), apo (red triangle) and holo (blue circle) forms of α-LA. (C) *In situ* TPE-TPP assay of molten globule (black open circle), apo (blue circle), holo (red triangle), and amyloid fibril-forming RCM α-LA (black circle). (D) TEM images of the holo form of α-LA and RCM α-LA fibrils formed in the presence of TPE-TPP. 20 μM of dye was used for all fluorescence assays. For TPE-TPP, the excitation and emission filters were 380/20 and 460/40 nm, respectively. The conditions for formation of the different α-LA aggregates are summarised in Table S1.

Full insight into the self-assembly of peptides and proteins and their role in disease requires both the identification and characterisation of early-stage aggregates and other conformational states adopted by the polypeptide chain along the pathway to the formation of amyloid fibrils. Although some progress has been made in this area, a better understanding of the nanoscale assembly of amyloid fibrils from normally soluble proteins is crucial for combating protein aggregation diseases as well as to exploit their potential benefits [20]. Previously one of us (Y.H.) reported that fluorogens with aggregation-induced emission (AIE) characteristics, such as BSPOTPE and TPE-TPP (Figure 1A, top panel) are non-fluorescent in solution but become highly fluorescent when they bind to amyloid fibrils of insulin and α-synuclein, respectively [21-23]. Furthermore, a competition experiment between ThT (Figure 1A, bottom panel) and TPE-TPP binding to α-synuclein fibrils indicated that TPE-TPP binds more efficiently (with a K_d of 4.36 μM) to the same site(s) as that of ThT (whose K_d is 8.48 μM) [21]. As derivatives of tetraphenylethene (TPE), a typical AIE luminogen, the emission of these dyes is triggered by the restriction of intramolecular motions (RIM) of the phenyl rotors in their aggregated form [24]. Additionally, in their aggregated state the highly twisted nature of the molecular structure impedes π-π interactions, thereby displaying strong fluorescence [23,25]. Similarly, RIM of AIE can also be achieved upon binding to larger macromolecules such as proteins. Increasing viscosity, decreasing temperature and elevated pressure are further expected to influence RIM by slowing the intramolecular rotation and hence leading to stronger TPE-TPP fluorescence emission [23,26].

In the present study, we applied the aforementioned properties of TPE-TPP to investigate protein assembly and disassembly. We find that, upon interacting with protein molecules, emission from TPE-TPP can specifically monitor the process of ordered protein aggregation, such as amyloid fibril formation, even under solution conditions of acidic pH and elevated temperature. Compared to ThT, TPE-TPP is markedly more sensitive with regards to recognition of aged amyloid fibrils, and no self-quenching of fibril-associated fluorescence is observed in the presence of excess dye. In contrast, complete loss of ThT fluorescence was observed during extended incubation of hen egg white lysozyme (HEWL) and κ-casein fibrils. TPE-TPP fluorescence increases upon generation of oligomeric assemblies formed during the early-stage of protein aggregation, and displays a significant spectral shift upon binding to prefibrillar species. In addition, using a microplate-based *in situ* TPE-TPP fluorescence assay, we screened three different types of potential inhibitors of amyloid fibril formation acting at various stages of aggregation. In comparison to the routinely used amyloid probe ThT, TPE-TPP shows broader *in vitro* applicability to investigate ordered protein aggregation process.

EXPERIMENTAL SECTION

Materials. TPE-TPP was synthesized as described in the literature [21]. All other reagents (proteins, amino acids, chemicals, solvents, etc.) were purchased from Sigma Life Sciences and Sigma-Aldrich unless otherwise specified. Recombinant D76N β2m, αB-crystallin and α-synuclein were expressed and purified as described previously [27,28]. The determination of protein concentration is described in SI.

Amorphous aggregation. The change in light scattering at 350 nm was used to monitor amorphous aggregation of α-LA and hen egg white lysozyme (HEWL). Assay conditions are described in detail in Table S1 and Table S2. Assays were conducted in Nunc 96 well polypropylene microplates, sealed with transparency film, incubated at 37 °C and light scattering was monitored using a Biotek Synergy 2 microplate reader.

Amyloid fibril formation. The fibrillar aggregation of proteins was monitored in Greiner Bio-One 384-well microplates (Item No.: 784900, small volume, black, flat bottom and non-binding) using a Biotek Synergy 2 microplate reader. The conditions for fibril formation are described in detail in Tables S1-3. Transparent sealing film was used to prevent solvent evaporation. ThT fluorescence emission was measured using a 440/40 nm filter for excitation and a 485/20 nm filter for emission, while for TPE-TPP fluorescence, the 380/20 and 460/40 nm filters were used for excitation and emission, respectively, under the fibrillation conditions appropriate for each protein. Dye concentrations were 20 μM and 5 μM for *in situ* and *ex situ* assays, respectively. The TPE-TPP fluorescence assay potentially may be affected by a high-binding microplate, therefore all TPE-TPP and ThT fluorescence assays were performed using the aforementioned non-binding microplate.

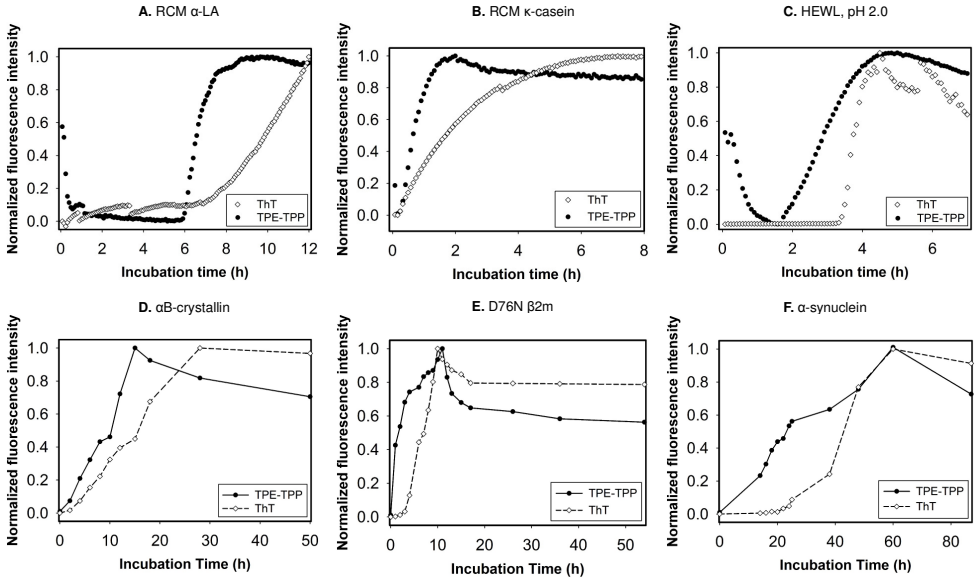

Figure 2. Comparison of the time-course aggregation profiles of six different amyloid fibril-forming proteins as monitored by ThT and TPE-TPP fluorescence. (A-C) *In situ* and (D-F) *ex situ* dye-binding fluorescence (normalized) profile of (A) 100 μM RCM α-LA, (B) 50 μM RCM κ-casein, (C) 35 μM HEWL at pH 2.0, (D) 10 μM αB-crystallin, (E) 40 μM D76N β2m and (F) 40 μM α-synuclein. TPE-TPP fluorescence intensity data are represented as solid circles and ThT fluorescence as open circles. 20 μM of dye was used for the *in situ* and 5 μM for the *ex situ* assays. For ThT, the excitation and emission filters were 440/40 and 485/20 nm, respectively. For TPE-TPP, the excitation and emission filters were 380/20 and 460/40 nm, respectively. Tables S2 and S3 summarize the amyloid fibril-forming conditions for each protein.

Fluorescence polarization. For FP experiments, amyloid fibrils were prepared according to the conditions outlined in Tables S1-3 using Greiner Bio-One 384-well microplates (small volume, black, flat bottom, and non-binding) with transparent sealing film. TPE-TPP was added to 20 μM prior to incubation of the protein. FP was recorded *in situ* with a CLARIOstar microplate reader (BMG Labtech) using the FP mode and a FP filter set of 380/20 nm for excitation and 485/20 nm for emission. The background fluorescence of TPE-TPP in the corresponding buffer solution under the respective protein fibrillation conditions was subtracted, and the change in FP values was expressed in milli-polarization units (ΔmP).

RESULTS AND DISCUSSION

TPE-TPP specifically monitors ordered protein aggregation. To determine whether TPE-TPP can distinguish between various types of protein aggregates, we measured the response of TPE-TPP against different aggregation pathways undertaken by the same protein under various experimental conditions. We first chose α-lactalbumin (α-LA) as the model protein because it is a well-characterized protein that can form a molten globule, amorphous aggregates and amyloid fibrils under the appropriate solution conditions (as described in Table S1) [29]. α-LA forms a characteristic molten globule state at pH 2.0, and Ca^{2+}-free (apo) and Ca^{2+}-bound (holo) α-LA form amorphous aggregates under reducing conditions. The rapid formation of amorphous aggregates upon reduction of α-LA was apparent from the change of the turbidity of the protein solution with time, as monitored via light scattering at 350 nm (Figure 1B). Reduced and carboxymethylated (RCM) α-LA, on the other hand, forms ordered amyloid fibrils under physiological conditions in the presence of Mg^{2+} and with agitation [30]. Figure 1C shows that TPE-TPP was weakly fluorescent in the presence of monomeric α-LA prior to incubation. Moreover, no enhancement of TPE-TPP emission was observed during the process of molten globule or amorphous aggregate formation. Interestingly, a significant rise in TPE-TPP fluorescence (in a sigmoidal manner) occurred during the fibrillar aggregation of RCM α-LA, implying that TPE-TPP is sensitive and selective to amyloid fibril formation. The formation of amorphous aggregates by holo α-LA, and fibrils by RCM α-LA in the presence of ThT and TPE-TPP was confirmed by transmission electron microscopy (TEM) with negative staining (Figure 1D).

Similar to α-LA, HEWL can form aggregates of different morphology as described in Table S2; for example, amyloid fibrils at pH 2.0 and amorphous aggregates at pH 12.2 [31,32]. Consistent with the response to the various forms of α-LA, TPE-TPP remained weakly fluorescent during the entire process of amorphous aggregation of HEWL, as monitored by light scattering at 350 nm. By contrast, TPE-TPP exhibited significant fluorescence enhancement, displaying a typical sigmoidal profile during the formation of lysozyme amyloid fibrils at pH 2.0 and 55 °C (Figure S1). Under such extreme pH and temperature conditions, ThT is unstable [33,34].

Moreover, we observed that ThT fluorescence intensity underwent major fluctuation even after mature fibrils had formed (see below). In addition to chemical reduction and the exposure to extreme pH conditions, heat can also denature proteins and induce aggregate formation. Both ThT and TPE-TPP fluorescence remained almost unchanged in the presence of bovine serum albumin (BSA) before and after heating to 95 °C, pH 7.4, i.e. conditions that induce the formation of disordered amorphous aggregates of this protein (Figure S2).

Observing prefibrillar/oligomeric species during protein aggregation. As TPE-TPP shows specific binding to amyloid fibrils over amorphous aggregates, we next investigated its application to follow the kinetics of protein aggregation, specifically amyloid fibril formation by RCM α-LA (Figure 2). RCM α-LA was incubated with TPE-TPP and ThT inde-

pendently, and the change in TPE-TPP and ThT fluorescence was monitored over time. TPE-TPP fluorescence intensity decreased significantly during the first 30 minutes of incubation and remained constant for the first 5.5 h (Figure 2A). The fluorescence emission of TPE-TPP then increased dramatically reaching a plateau after 8 h of incubation. The commensurate experiment with ThT showed constant weak fluorescence for the first 7 h of incubation and then a slow increase such that it had not reached a plateau even after 12 h of incubation. Thus, there is a notable difference in the fluorescence profiles of both dyes in the presence of aggregating RCM α-LA. It appears that TPE-TPP fluorescence is more sensitive to the early species formed prior to the formation of fibrillar entities than those detected by ThT fluorescence.

To examine whether this is a general phenomenon, i.e. that TPE-TPP can monitor species formed early during protein fibrillation, we extended our studies to other amyloid fibril-forming proteins. Similar to RCM α-LA, TPE-TPP fluorescence intensity exhibited an initial decrease during the incubation period and then rose at an earlier time point than ThT during the fibrillation process of RCM κ-casein and HEWL (Figure 2B,C). In each of the three cases examined, the dyes were mixed with the proteins before aggregation commenced (i.e. *in situ* assay; Figures 2A-C). To rule out the possibility of the early increase in TPE-TPP fluorescence being due to a change in the rate of aggregation as a result of the interaction of AIE molecules, we also conducted studies involving the addition of the dyes to aliquots collected at different time points during the aggregation process (i.e. *ex situ* assay). The molecular chaperone protein αB-crystallin, D76N β2-microglobulin (β2m), a naturally occurring amyloidogenic variant of β2m (the protein involved in dialysis-related amyloidosis), and the synucleinopathies-associated protein α-synuclein, were used in this work as they all readily form fibrils under the conditions tested [35-37]. Consistent with the *in situ* assays, TPE-TPP showed fluorescence enhancement with these proteins at time points earlier than ThT (Figure 2D-F). Both the *in situ* and *ex situ* assay results clearly indicate that TPE-TPP is capable of detecting early stage/prefibrillar aggregating species which are not observed using ThT.

Spectral shift of TPE-TPP fluorescence with different protein species. The normalized emission spectrum of TPE-TPP exhibited a significant blue and red shift when it was mixed with purified prefibrillar and fibrillar α-LA, respectively, compared to that in the presence of the monomeric species (Figure 3A). The emission spectrum of TPE-TPP exhibited an emission maximum at 474 nm when mixed with RCM α-LA monomers, which shifted to 460 nm with prefibrillar RCM α-LA. In contrast, the emission maximum was red-shifted to 484 nm when mixed with purified RCM α-LA fibrils. The early-stage species detected at around 6 h by TPE-TPP (Figure 2A)

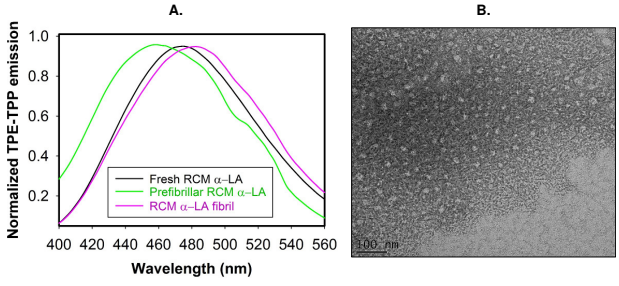

Figure 3. Fluorescence emission spectrum of TPE-TPP upon binding to different forms of α-LA. (A) Normalized TPE-TPP fluorescence emission upon binding to fresh, non-aggregated (black curve), prefibrillar (green curve) and fibrillar (magenta curve) species of RCM α-LA. (B) TEM image of RCM α-LA prefibrillar species; scale = 100 nm. The TPE-TPP fluorescence emission spectrum was measured with excitation at 350 nm.

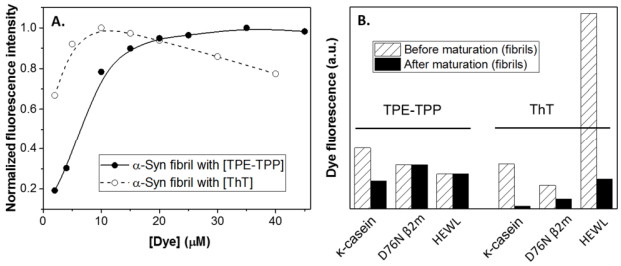

Figure 4. Fluorescence change at different dye: fibril stoichiometry, and upon maturation of fibrils. (A) Change in fluorescence intensity with increasing dye-to-protein concentration ratio. Protein: 10 μM mature α-synuclein fibrils. The data of dye with mature HEWL fibrils are shown in Figure S4. TPE-TPP fluorescence shown by solid black circle and line, and ThT fluorescence is represented by an open black circle and dashed line (B) Fibril maturation-induced quenching of ThT and TPE-TPP fluorescence. Actual TPE-TPP and ThT fluorescence intensity upon binding to non-incubated 2-day (hollow bar) and upon ageing (solid black bar) protein fibrils, as indicated in the figure. The concentration of the proteins and dyes was each 10 μM.

was separated and purified from other RCM α-LA forms using native agarose gel electrophoresis and an Ultrafree®-DA centrifugal unit, respectively. The Ultrafree®-DA unit utilises centrifugal force and a microporous membrane to disperse the agarose gel matrix, thereby allowing recovery of the protein. The non-fibrillar spherical morphology of the prefibrillar RCM α-LA was confirmed by TEM (Figure 3B). A similar hypsochromic shift of TPE-TPP fluorescence emission maximum to ~465 nm was also observed when it was mixed with prefibrillar D76N β2m, but no significant change in the emission maximum occurred when mixed with fibrillar D76N β2m compared to the monomeric form of the protein (Figure S3). Thus, such spectral shifts in TPE-TPP fluorescence emission can be used to differentiate between various protein forms.

Absence of self-quenching and fibril maturation-induced fluorescence quenching. Younan and Viles reported that an excess of ThT can cause quenching of fluorescence upon binding to amyloid β-peptide fibrils [38]. To test whether TPE-TPP has the same behaviour, the dye-to-protein fibril ratio was increased, and fluorescence spectra were recorded. The concentration of the pre-formed protein fibrils was fixed at 10 μM and the concentration of dye (ThT or TPE-TPP) was altered from 1 to 40-50 μM. Consistent with the above study, ThT fluorescence decreased once the dye-to-protein concentration ratio was greater than 1:1 for both HEWL and α-synuclein fibrils (Figure 4A and S4). In contrast, the TPE-TPP fluorescence intensity increased proportionally with the increase in the dye-to-protein fibril ratio, reaching a plateau when the molar ratio reached 2:1 dye: fibrillar protein. No self-quenching of fluorescence occurred even when the dye-to-protein fibril ratio was greater than 4:1 for both fibrillar species.

In addition to the problems associated with self-quenching, we found that ThT only exhibited appreciable fluorescence with fibrils of κ-casein, D76N β2m and HEWL that were freshly prepared. In order to examine whether this is also a limitation of TPE-TPP, the proteins were incubated under conditions conducive to fibril formation for 48 h. At the end of the incubation, ThT and TPE-TPP fluorescence spectra of an aliquot from each protein was measured (before maturation), and the remainder of the sample was then incubated at room temperature for an additional 7-30 days and measured (after

maturation). We measured an ~18 fold decrease in ThT fluorescence signal in the case of 30-day aged RCM κ-casein fibrils (Figure 4B). An ~7- and 2.4-fold loss of ThT fluorescence signal occurred for 7-day and 30-day-old HEWL and D76N β2m fibrils, respectively (Figure 4B). On the contrary, no notable reduction of TPE-TPP fluorescence was observed between the fibrils formed at 48 h and aged forms (7-day-old HEWL and 30-day-old D76N β2M fibrils). However, a ~2-fold signal loss was observed in the case of 30-day aged RCM κ-casein fibrils. Hence, unlike ThT, TPE-TPP bound more efficiently to aged HEWL, D76N β2m and RCM κ-casein fibrillar species.

This self-quenching effect makes it difficult to measure the rate of fibril formation accurately using ThT fluorescence. It is also noteworthy to speculate that the extended lag phase in the kinetic curves could be attributed to quenching of ThT fluorescence during the early phase of fibrillation, i.e. when the amyloid fibril content is much lower than the dye concentration. As a result, this may lead to inaccuracies in the assessment of the lag phase of the reaction when using *in situ* ThT assays. Similar to our observation, other studies have also noted that fibril morphology can significantly affect ThT fluorescence [33,39].

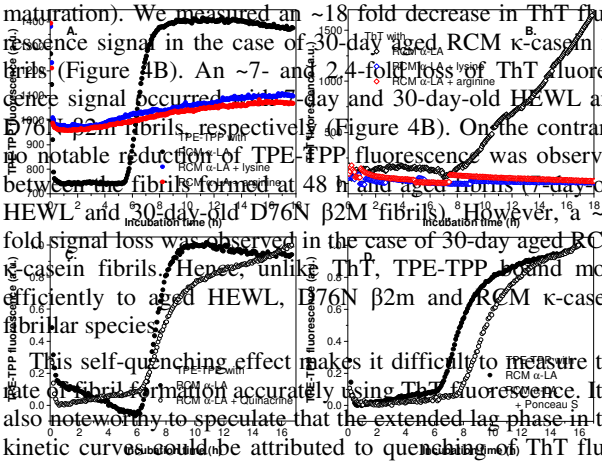

Figure 5. Screening and evaluation of potential inhibitors for amyloid fibril formation as monitored by TPE-TPP fluorescence. (A) TPE-TPP fluorescence intensity of 125 μM RCM α-LA in the absence (black circle) and presence of 10 mM lysine (blue circle) or 10 mM arginine (red circle). (B) ThT fluorescence intensity of 125 μM RCM α-LA in the absence (black circle) and presence of 10 mM lysine (blue diamond) or 10 mM arginine (open red circle). Normalized TPE-TPP fluorescence intensity of (C) 125 μM RCM α-LA in the absence (solid circle) and presence of 10 μM Quinacrine (open circle), and (D) 125 μM RCM α-LA in the absence (solid circle) and presence of 10 μM Ponceau S (open circle).

Monitoring the effects of amyloid fibril inhibitors. Using a fluorescence-based approach for rapid screening of potential therapeutic agents that can act on various stages of the amyloid fibril-forming pathway is a challenging task because of the limitations of routinely used amyloid probes. Since TPE-TPP can follow the kinetics and reveal the early-stage processes during protein fibrillation, the effect of small molecules on amyloid fibril formation was investigated. We examined the effects of lysine and arginine, well-described potent inhibitors of protein aggregation [40-42], on RCM α-LA fibrillation using TPE-TPP and ThT fluorescence assays (Figure 5A,B). No significant increase in TPE-TPP fluorescence was observed when RCM α-LA was incubated in the presence of lysine or arginine, suggesting complete suppression of the fibrillation process (Figure 5A). The inhibitory effect of lysine and arginine was confirmed using a ThT-based fluorescence assay (Figure 5B).

Quinacrine, a tricyclic acridine compound, has also been extensively studied for its potential treatment of prion diseases and has been reported to inhibit amyloid β peptide fibrillation [43-45]. We investigated the effect of quinacrine on RCM α-LA amyloid fibril formation via TPE-TPP fluorescence (Figure 5C). Whilst quinacrine did not completely inhibit fibril formation by RCM α-LA, it slowed its rate of fibril formation and resulted in a change in fibril morphology, as evident by TEM (Figure S5A). When incubated in the presence of quinacrine, RCM α-LA amyloid fibrils (*cf* Figure 1D) were much shorter with more globular and spherical aggregates when quinacrine was not present (Figure S5A). In addition, Ponceau S, a diazo dye that is regularly used as a reversible stain for the detection of proteins in Western blotting [46], modulates RCM α-LA fibril formation (Figure 5D). When monitored by TPE-TPP fluorescence, fibril formation by RCM α-LA in the presence of Ponceau S had an extended lag phase by about 1.5 h compared to when Ponceau S was not present. By prolonging the lag phase, the diazo dye acts on the early stage of the protein's aggregation, most likely by altering the fibrillation pathway resulting in the formation of unstable fibrillar structures, as observed by TEM (Figure S5B).

The formation of amyloid fibrils can be prevented in a number of ways: by stabilizing the native structure of the precursor protein or peptide, by inhibiting or altering oligomerization during the early stage of fibrillation and by modulating or suppressing fibril elongation. Identifying distinct inhibitors for each of these cases can be a difficult process. The TPE-TPP fluorescence profiles of RCM α-LA in the presence of arginine and lysine suggest that both positively charged amino acids stabilised monomeric RCM α-LA, preventing it from further aggregation. Ponceau S, a diazo compound, modulated the prefibrillar RCM α-LA form leading to the formation of unstable fibrillar species, thereby altering the normal RCM α-LA fibrillation pathway as indicated by the extended lag-phase. Quinacrine appears to attenuate the rate of RCM α-LA amyloid formation, producing shorter fibrillar structures. Thus, by monitoring the TPE-TPP fluorescence associated with fibril formation, we are able to draw conclusions on the possible inhibitory mechanism of different fibril inhibitors.

Fluorescence polarization for monitoring the oligomeric pathway during protein assembly. In addition to measuring the change in fluorescence intensity during amyloid fibril formation, we recorded the change in fluorescence polarization (FP) of TPE-TPP. FP reflects the mobility of the emitting species such that when the fluorescent molecule binds to a small target it freely rotates and has small FP values. However, when the fluorescent molecule binds to a large molecule, its rotation/mobility slows and its FP value increases. The alteration in the FP value is therefore proportional to the relative mass of the object to which it binds [1,47-49]. The change in FP of TPE-TPP during the fibrillation of RCM α-LA, RCM κ-casein and insulin was therefore measured to examine whether it could be used to monitor amyloid fibril formation by these proteins.

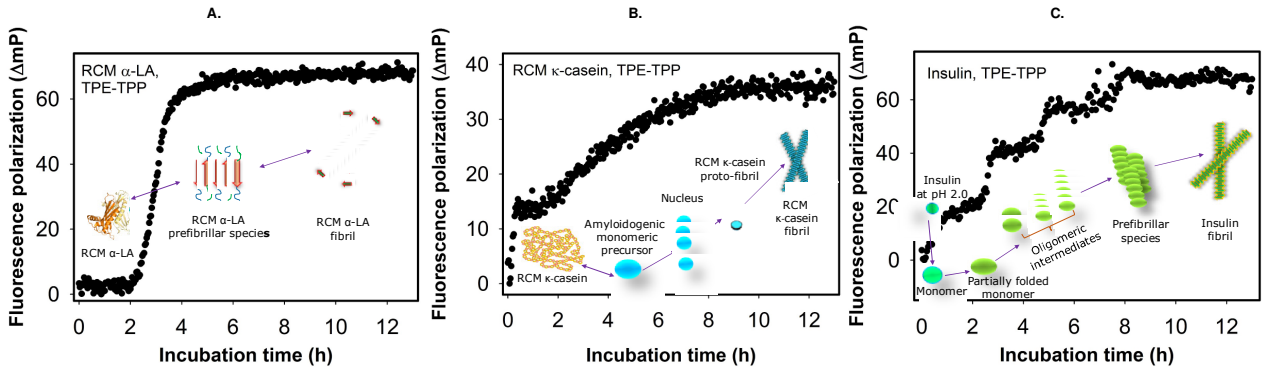

Figure 6. Protein fibril formation monitored by FP. Time-dependent change in FP (ΔmP) of TPE-TPP (20 μM) during amyloid fibril formation of (A) 125 μM RCM α-LA, (B) 50 μM RCM κ-casein and (C) 200 μM insulin.

RCM α-LA (monomeric mass 14.7 kDa) follows classical nucleation-dependent polymerization as apparent from its sigmoidal kinetic fluorescence curve [30]. Starting from monomers, soluble oligomers with increasing mass were formed after 2 h of incubation, as reflected by the steep increase of the FP. Afterwards, rigid insoluble fibrils were formed with FP reaching a maximum value and staying constant over the next 8 h (Figure 6A). On the other hand, RCM κ-casein (monomeric mass ~19 kDa) forms amyloid fibrils via a different mechanism with the absence of a significant lag phase. In solution at 25°C, RCM κ-casein occurs as a spherical particle with a weight-average molecular mass of ~1180 kDa [50]. Consistent with the difference in molecular mass, the FP of RCM κ-casein prior to incubation was higher than that of RCM α-LA (Figure 6B). At 37 °C and neutral pH, RCM κ-casein reassembles into fibrillar structures [50-52]. Amyloid fibril formation by RCM κ-casein involves the dissociation of its spherical, oligomeric form into a monomeric amyloidogenic precursor, which then undergoes rapid aggregation to form a nucleus from which rigid, rod-like amyloid fibrils develop [51,52]. Bovine insulin (monomeric mass 5.8 kDa) forms amyloid fibrils at acidic pH (pH 2.0) and elevated temperature (60 °C). Insulin exists as a dimer at acidic pH, which rapidly dissociates to monomer at higher temperature followed by a conformational change. The partially unfolded monomers associate with each other to form oligomeric intermediates including dimers, tetramers and hexamers [53]. Hexamers have been reported to be a critical prefibrillar intermediate in the formation of mature amyloid fibrils [54]. The progression from monomer to dimer, tetramer, hexamer and then to insulin amyloid fibril is observed by the step-wise increase, each of around similar magnitude in the FP of TPE-TPP (Figure 6C). Thus, TPE-TPP-based FP measurements can map the oligomeric assemblies, whilst monitoring the fibrillar assembly, of a variety of amyloid fibril-forming protein *in situ*. Moreover, because FP is less dependent on the dye concentration, its signal remained constant after reaching the plateau, whereas a decrease in fluorescence intensity is often observed after the formation of insoluble fibrils (*cf* Figure 2).

Mechanism of TPE-TPP binding to amyloid fibrils. TPE-TPP is non-fluorescent in buffer solution owing to the aggregation-induced emission property of its TPE core as the fluorophore. Once bound to a macromolecule such as a protein, the intramolecular motions of the peripheral phenyl rings of TPE are restricted, and the dye becomes emissive [23]. In contrast to ThT, TPE-TPP does not have any electron donating or accepting groups conjugated to its fluorogenic unit (Figure 1A). Therefore, it is unlikely to undergo the twisted intramolecular charge transfer mechanism ascribed to ThT fluorescence [55,56].

Immediate TPE-TPP fluorescence was observed following incubation with all the freshly prepared (non-aggregated) proteins used in this study, i.e. α-LA, HEWL, D76N β2m, RCM κ-casein, αB-crystallin and α-synuclein. However, no further enhancement of TPE-TPP fluorescence occurred when the proteins were induced to form the molten globule state or amorphous aggregates. In contrast, TPE-TPP exhibited significant fluorescence enhancement when incubated with proteins as they underwent fibril formation. TPE-TPP is like ThT in binding preferentially to the cross β-sheet structure that is characteristic of amyloid fibrils. The exact mechanism of ThT interaction with amyloid fibrils is a matter of debate. Potentially, TPE-TPP could interact with hydrophobic residues and emit fluorescence. Molten globule states and amorphous aggregates both have significant exposed hydrophobicity but they do not have well-defined β-sheet conformations in place and are much more dynamic and less-structured entities than the highly structured amyloid fibrils and hence do not provide significant physical constraint to enhance TPE-TPP fluorescence. Thus, TPE-TPP is a fluorescent dye that selectively monitors *in vitro* amyloid fibril formation, but not molten globule states or amorphous (disordered) protein aggregates.

Following incubation, TPE-TPP exhibited *in situ* and *ex situ* fluorescence enhancement much earlier than ThT during protein fibril formation, suggesting that TPE-TPP can interact with prefibrillar aggregates but not interfere with aggregate formation. Furthermore, a significant blue shift in the fluorescence emission spectrum of TPE-TPP occurred in the presence of prefibrillar, oligomeric species compared to native forms of the same protein (Figures 3A and S3). The blue shift observed in the fluorescence emission spectrum when TPE-TPP interacted with prefibrillar protein species also occurs for TPE-TPP in the most viscous solvent, glycerol, when compared with less viscous solvents or solvents with greater polarity, and is accompanied by an increase in fluorescence intensity at the wavelength emission maximum (Figures S6 and S7). For example, the emission maximum of TPE-TPP is ~470 nm in ethylene glycol but is shifted to ~430 nm in 25% v/v glycerol and is enhanced in intensity (Figure S6). Only a small change in Stokes shift is observed when the glycerol percentage is increased from 25% to 100% v/v but a large and linear increase in fluorescence intensity occurs (Figures S6 and S7). Such a viscous and rigid local environment could restrict the

intramolecular motions of the excited species and may enable the transition of the excited species from a higher energy level to the ground state, resulting in a blue shift of the fluorescence spectrum. By extrapolation, potentially these observations imply that the presence of soluble oligomeric assemblies enhances the local viscosity in the surrounding environment of the TPE-TPP dye. This is consistent with literature reports that the formation of early-stage soluble oligomeric assemblies increases the viscosity of the local environment during protein assembly [57-61].

A red shift in TPE-TPP emission upon binding to RCM α-LA mature fibrils also occurred, which was not observed with D76N β2m fibrils (Figure 3A and S3), suggesting that TPE-TPP can also detect morphological variations in amyloid fibrils. When the dye molecules bind to the mature fibrils of ordered structure, they may have to adjust their conformation, for example via rearranging the dihedral angle between the phenyl rings and the central double bond of TPE, to fit into the binding site. As a result, a red shift in the spectrum would be observer.

TPE-TPP can thus recognise and bind to various protein forms with different specificity resulting in spectral changes. Importantly, by monitoring such changes in the TPE-TPP emission spectrum, it is feasible to differentiate between non-aggregated, pre- and fibrillar protein forms. Although complementary assays based on TEM or atomic force microscopy are always useful to characterize protein morphology, the possibilities of using TPE-TPP fluorescence provides a rapid and convenient way to differentiate proteins adopting different morphologies.

CONCLUSIONS

In summary, our work demonstrates that TPE-TPP has many advantages over ThT in its applicability to monitor amyloid fibril formation. TPE-TPP detects the emergence of prefibrillar aggregates, is more robust in monitoring amyloid fibril formation at highly acidic pH and/or high temperatures, and it can be used in the presence of exogenous potential inhibitors, including in high-throughput screening. It also does not undergo self-quenching when present in excess compared to the concentration of the fibrils, and retains its fluorescence properties when used with aged amyloid fibrils. Furthermore, TPE-TPP fluorescence can monitor the oligomeric pathway of a protein during amyloid fibril formation. Thus, we propose that in many respects, TPE-TPP is a superior dye for fluorescence-based detection and characterization of amyloid fibril aggregation.

ASSOCIATED CONTENT

Supporting Information

The Supporting Information is available free of charge on the ACS Publications website.
Experimant section, aggregation conditions of different proteins, fluorescence response to lysozyme and BSA aggregation, TEM images of fibrils formed in the presence of inhibitors, excitation and emission spectra in solvents with different viscosity and polarity and the solvatochromism plot (PDF).

AUTHOR INFORMATION

Corresponding Author

* Y.Hong@latrobe.edu.au
* john.carver@anu.edu.au

Author Contributions

M.K., Y.H. and J.C. designed the experiments; M.K. and Y.H. performed the experiments; M.K., Y.H., D.T., H.E. and J.C. analyzed the data; M.K., Y.H. and J.C. wrote the manuscript with feedback from the other authors.

Notes

The authors declare no competing financial interests.

ACKNOWLEDGMENT

This work was supported by a National Health and Medical Research Council project grant to J.C. (#1068067), and an Australian Research Council DECRA award (#DE170100058) and Melbourne Neuroscience Institute Interdisciplinary Seed Funding to Y.H. Y.H. thanks the support of Bruce Stone Fellowship from La Trobe University and a McKenzie Fellowship from The University of Melbourne. We also thank the Centre for Advanced Microscopy, the ANU node of the Australian Microscopy and Microanalysis Research Facility, for transmission electron microscopy.

ABBREVIATIONS

AIE: aggregation-induced emission, AGE: agarose gel electrophoresis, a.u.: arbitrary unit, BSA: bovine serum albumin, D76N β2m: D76N variant of β2-microglobulin, EX: excitation, EM: emission, FP: fluorescence polarization, HEWL: hen egg white lysozyme, O.D.: optical density, RCM: reduced and carboxymethylated, RIM: restriction of intramolecular motions, ThT: thioflavin T, TPE-TPP: Bis(triphenylphosphonium) tetraphenylethene.

REFERENCES

(1) Lakowicz, J. R. *Principles of Fluorescence Spectroscopy*; 3 rd ed.; Springer:US, 2007.
(2) Sipe, J. D.; Cohen, A. S. *J Struct Biol* **2000**, *130*, 88-98.
(3) Sipe, J. D.; Benson, M. D.; Buxbaum, J. N.; Ikeda, S.-i.; Merlini, G.; Saraiva, M. J. M.; Westermark, P. *Amyloid* **2012**, *19*, 167-170.
(4) Fowler, D. M.; Koulov, A. V.; Balch, W. E.; Kelly, J. W. *Trends Biochem Sci* **2007**, *32*, 217-224.
(5) Chiti, F.; Dobson, C. M. *Annu Rev Biochem* **2006**, *75*, 333-366.
(6) Hardy, J.; Selkoe, D. J. *Science* **2002**, *297*, 353-356.
(7) Glabe, C. C. *Subcell Biochem* **2005**, *38*, 167-177.
(8) Arosio, P.; Knowles, T. P. J.; Linse, S. *Phys Chem Chem Phys* **2015**, *17*, 7606-7618.
(9) LeVine, H., 3rd. *Protein Sci* **1993**, *2*, 404-410.
(10) Levine, H. *Arch Biochem Biophys* **1997**, *342*, 306-316.
(11) Groenning, M.; Olsen, L.; van de Weert, M.; Flink, J. M.; Frokjaer, S.; Jorgensen, F. S. *J Struct Biol* **2007**, *158*, 358-369.
(12) Khurana, R.; Uversky, V. N.; Nielsen, L.; Fink, A. L. *J Biol Chem* **2001**, *276*, 22715-22721.
(13) Ashburn, T. T.; Han, H.; McGuinness, B. F.; Lansbury, P. T., Jr. *Chem Biol* **1996**, *3*, 351-358.
(14) Hammarstrom, P.; Simon, R.; Nystrom, S.; Konradsson, P.; Aslund, A.; Nilsson, K. P. *Biochemistry* **2010**, *49*, 6838-6845.
(15) Viriot, M. L.; Carre, M. C.; Geoffroy-Chapotot, C.; Brembilla, A.; Muller, S.; Stoltz, J. F. *Clin Hemorheol Microcirc* **1998**, *19*, 151-160.
(16) Sackett, D. L.; Wolff, J. *Anal Biochem* **1987**, *167*, 228-234.
(17) Teoh, C. L.; Su, D.; Sahu, S.; Yun, S. W.; Drummond, E.; Prelli, F.; Lim, S.; Cho, S.; Ham, S.; Wisniewski, T.; Chang, Y. T. *J Am Chem Soc* **2015**, *137*, 13503-13509.
(18) Celej, M. S.; Jares-Erijman, E. A.; Jovin, T. M. *Biophys J* **2008**, *94*, 4867-4879.
(19) Reinke, A. A.; Abulwerdi, G. A.; Gestwicki, J. E. *Chembiochem* **2010**, *11*, 1889-1895.
(20) Rambaran, R. N.; Serpell, L. C. *Prion* **2008**, *2*, 112-117.
(21) Leung, C. W. T.; Guo, F.; Hong, Y. N.; Zhao, E. G.; Kwok, R. T. K.; Leung, N. L. C.; Chen, S. J.; Vaikath, N. N.; El-Agnaf, O. M.; Tang, Y. H.; Gai, W. P.; Tang, B. Z. *Chem Commun* **2015**, *51*, 1866-1869.

(22) Hong, Y.; Meng, L.; Chen, S.; Leung, C. W.; Da, L. T.; Faisal, M.; Silva, D. A.; Liu, J.; Lam, J. W.; Huang, X.; Tang, B. Z. *J Am Chem Soc* **2012**, *134*, 1680-1689.
(23) Yuning, H. *Methods Appl in Fluoresc* **2016**, *4*, 022003.
(24) Hong, Y.; Lam, J. W. Y.; Tang, B. Z. *Chem Soc Rev* **2011**, *40*, 5361-5388.
(25) Yuan, W. Z.; Lu, P.; Chen, S.; Lam, J. W. Y.; Wang, Z.; Liu, Y.; Kwok, H. S.; Ma, Y.; Tang, B. Z. *Adv Mater* **2010**, *22*, 2159-2163.
(26) Hong, Y.; Lam, J. W. Y.; Tang, B. Z. *Chem Commun* **2009**, 4332-4353.
(27) Valleix, S.; Gillmore, J. D.; Bridoux, F.; Mangione, P. P.; Dogan, A.; Nedelec, B.; Boimard, M.; Touchard, G.; Goujon, J. M.; Lacombe, C.; Lozeron, P.; Adams, D.; Lacroix, C.; Maisonobe, T.; Plante-Bordeneuve, V.; Vrana, J. A.; Theis, J. D.; Giorgetti, S.; Porcari, R.; Ricagno, S., et al. *N Engl J Med* **2012**, *366*, 2276-2283.
(28) Horwitz, J.; Huang, Q. L.; Ding, L.; Bova, M. P. *Methods Enzymol* **1998**, *290*, 365-383.
(29) Carver, J. A.; Lindner, R. A.; Lyon, C.; Canet, D.; Hernandez, H.; Dobson, C. M.; Redfield, C. *J Mol Biol* **2002**, *318*, 815-827.
(30) Kulig, M.; Ecroyd, H. *Biochem J* **2012**, *448*, 343-352.
(31) Wang, S. S.; Liu, K. N.; Lee, W. H. *Biophys Chem* **2009**, *144*, 78-87.
(32) Kumar, S.; Ravi, V. K.; Swaminathan, R. *Biochim Biophys Acta* **2009**, *1794*, 913-920.
(33) Freire, S.; de Araujo, M. H.; Al-Soufi, W.; Novo, M. *Dyes Pigm* **2014**, *110*, 97-105.
(34) Hackl, E. V.; Darkwah, J.; Smith, G.; Ermolina, I. *Eur Biophys J Biophy* **2015**, *44*, 249-261.
(35) Drueke, T. B. *Nephrol Dial Transplant* **2000**, *15 Suppl 1*, 17-24.
(36) Casey, T. T.; Stone, W. J.; DiRaimondo, C. R.; Page, D. L.; Gorevic, P. D. *Arthritis Rheum* **1986**, *29*, 1170.
(37) Marques, O.; Outeiro, T. F. *Cell Death Dis* **2012**, *3*, e350.
(38) Younan, N. D.; Viles, J. H. *Biochemistry* **2015**, *54*, 4297-4306.
(39) Lindberg, D. J.; Wranne, M. S.; Gilbert Gatty, M.; Westerlund, F.; Esbjörner, E. K. *Biochem Bioph Res Co* **2015**, *458*, 418-423.
(40) Das, U.; Hariprasad, G.; Ethayathulla, A. S.; Manral, P.; Das, T. K.; Pasha, S.; Mann, A.; Ganguli, M.; Verma, A. K.; Bhat, R.; Chandrayan, S. K.; Ahmed, S.; Sharma, S.; Kaur, P.; Singh, T. P.; Srinivasan, A. *PloS one* **2007**, *2*, e1176.
(41) Sinha, S.; Lopes, D. H. J.; Du, Z.; Pang, E. S.; Shanmugam, A.; Lomakin, A.; Talbiersky, P.; Tennstaedt, A.; McDaniel, K.; Bakshi, R.; Kuo, P.-Y.; Ehrmann, M.; Benedek, G. B.; Loo, J. A.; Klärner, F.-G.; Schrader, T.; Wang, C.; Bitan, G. *J Am Chem Soc* **2011**, *133*, 16958-16969.
(42) Schrader, T.; Bitan, G.; Klarner, F.-G. *Chem Commun* **2016**, *52*, 11318-11334.
(43) Barret, A.; Tagliavini, F.; Forloni, G.; Bate, C.; Salmona, M.; Colombo, L.; De Luigi, A.; Limido, L.; Suardi, S.; Rossi, G.; Auvre, F.; Adjou, K. T.; Sales, N.; Williams, A.; Lasmezas, C.; Deslys, J. P. *J Virol* **2003**, *77*, 8462-8469.
(44) Kumar, M.; Sarkar, N.; Dubey, V. K. *Protein Pept Lett* **2012**, *19*, 826-831.
(45) Dolphin, G. T.; Chierici, S.; Ouberai, M.; Dumy, P.; Garcia, J. *Chembiochem* **2008**, *9*, 952-963.
(46) Al-Amoudi, M. S.; Salman, M.; Al-Majthoub, M. M.; Adam, A. M. A.; Alshanbari, N. A.; Refat, M. S. *Res Chem Intermediat* **2015**, *41*, 3089-3108.
(47) Du, Y. *Methods Mol Biol* **2015**, *1278*, 529-544.
(48) Jameson, D. M.; Seifried, S. E. *Methods* **1999**, *19*, 222-233.
(49) Du, Y.; Masters, S. C.; Khuri, F. R.; Fu, H. *J Biomol Screen* **2006**, *11*, 269-276.
(50) Farrell, H. M., Jr.; Cooke, P. H.; Wickham, E. D.; Piotrowski, E. G.; Hoagland, P. D. *J Protein Chem* **2003**, *22*, 259-273.
(51) Ecroyd, H.; Koudelka, T.; Thorn, D. C.; Williams, D. M.; Devlin, G.; Hoffmann, P.; Carver, J. A. *J Biol Chem* **2008**, *283*, 9012-9022.
(52) Ecroyd, H.; Thorn, David C.; Liu, Y.; Carver, John A. *Biochem J* **2010**, *429*, 251-260.
(53) Bekard, I. B.; Dunstan, D. E. *Biophys J* **2009**, *97*, 2521-2531.
(54) Groenning, M.; Frokjaer, S.; Vestergaard, B. *Curr Protein Pept Sci* **2009**, *10*, 509-528.
(55) Ghosh, R.; Palit, D. K. *Chemphyschem* **2014**, *15*, 4126-4131.
(56) Amdursky, N.; Erez, Y.; Huppert, D. *Acc Chem Res* **2012**, *45*, 1548-1557.
(57) Liu, J.; Nguyen, M. D.; Andya, J. D.; Shire, S. J. *J Pharm Sci* **2005**, *94*, 1928-1940.
(58) Amin, S.; Barnett, G. V.; Pathak, J. A.; Roberts, C. J.; Sarangapani, P. S. *Curr Opin Colloid Interface Sci* **2014**, *19*, 438-449.
(59) Nicoud, L.; Lattuada, M.; Yates, A.; Morbidelli, M. *Soft Matter* **2015**, *11*, 5513-5522.
(60) Connolly, Brian D.; Petry, C.; Yadav, S.; Demeule, B.; Ciaccio, N.; Moore, Jamie M.; Shire, Steven J.; Gokarn, Yatin R. *Biophys J* **2012**, *103*, 69-78.
(61) Perng, M. D.; Huang, Y. S.; Quinlan, R. A. *Methods Enzymol* **2016**, *569*, 155-175.

Table of Contents